SUPPLEMENTARY MATERIAL

Differential inhibitor sensitivity of anaplastic lymphoma kinase variants found in neuroblastoma

Scott C. Bresler, Andrew C. Wood, Elizabeth A. Haglund, Joshua Courtright, Lili T. Belcastro, Jefferson S. Plegaria, Kristina Cole, Yana Toporovskaya, Huaqing Zhao, Erica L. Carpenter, James G. Christensen, John M. Maris, Mark A. Lemmon, and Yaël P. Mossé

Supplementary Methods

Supplementary References

SUPPLEMENTARY METHODS

DNA constructs and retrovirus production. Mutated and wild-type ALK cDNAs were cloned into the pCMV-XLS vector and subcloned into the retroviral vector MigR1, which also directs EGFP expression. Infection of retinal pigment epithelial cells (RPE1) that express telomerase (hTERT-RPE1) was performed as follows: Phoenix Ampho cells (Oribigen – RVC-10001) were plated ~ 500,000 cells in a 6 well plate in DMEM media with 10% FBS, 1% Pen/Strep, Gentamicin. Twenty-four hours after plating (~50% confluent), Phoenix cells were transfected with the ALK expression constructs using a 6:1 dilution of Fugene:plasmid DNA, and virus-containing medium was harvested 48 hours later. hTERT-RPE1 cells were plated at ~500,000 cells per well in a 6 well plate, and growth medium was replaced with 'virus cocktail' (2 ml growth medium, 1ml filtered (0.45μm) viral media from Phoenix cells, 4μg/ml Polybrene (Santa Cruz)) and incubated overnight. Viral medium then replaced with fresh growth medium, and hTERT-RPE1 cells were incubated for 48 hours before sorting by flow cytometry for EGFP-positive cells.

Production and purification of recombinant ALK-TKD proteins.
DNA encoding ALK residues 1090-1416, together with an N-terminal hexahistidine tag, was subcloned into pFastBac-1 (Invitrogen) for expression of histidine-tagged recombinant ALK-TKDs in Sf9 cells. Recombinant baculovirus was generated using the Bac-to-Bac system (Invitrogen). Sf9 cells were infected with recombinant virus for 3 days at 27˚C, harvested by centrifugation, and lysed by sonication. His-tagged protein was recovered from the lysis supernatant using NTA-Ni-agarose beads (Qiagen). After elution from NTA-Ni beads, ALK-TKD was dephosphorylated by incubation with 1μM YopH phosphatase (*S1*) for 12 hours at 4˚C to reverse spontaneous autophosphorylation that occurs within Sf9 cells during expression. ALK-TKD was then flowed over a cation exchange column (to remove YopH), exchanged into buffer containing 1M $(NH_4)_2SO_4$, and applied to a butyl sepharose column (GE Healthcare). Protein was eluted with a 20 column-volume linear gradient to 0M $(NH_4)_2SO_4$. ALK-TKD fractions were pooled and concentrated, and gel filtered using a Superdex 200 column (GE Healthcare) equilibrated in 25mM HEPES pH 7.4, 150mM NaCl, 4mM DTT. Mass spectrometry confirmed that dephosphorylation of the starting material was complete. Protein concentrations were determined by absorbance at 280nm using the calculated extinction coefficient 39440$cm^{-1}M^{-1}$. Phosphorylated ALK-TKD for peptide-based assays was produced in 100mM HEPES pH 7.4, 150mM NaCl, 2mM DTT,10mM $MgCl_2$, 2mM ATP in the presence of lipid vesicles containing 10% DOGS-NTA-Ni (Avanti Polar Lipids) in a background of dioleoylphosphatidylcholine (Avanti Polar Lipids) prepared as described (*S2*) with a final concentration of 10μM DOGS-NTA-Ni (100μM total lipid). Full ALK-TKD autophosphosphorylation was achieved within 50mins (Fig. 4A, lower panel) under these conditions at 25˚C. Reactions were quenched where necessary by addition of EDTA to a final concentration of 20mM, followed by desalting under the conditions described above for gel filtration. EGFR-TKD was prepared as described (*S2*). Mass spectrometry-based phosphopeptide analysis confirmed that ALK-TKD autophosphorylation occurs at the expected sites within the activation loop, as well as additional sites.

***In vitro* protein and phosphoprotein detection.**
Each neuroblastoma cell line was cultured in ten T75 flasks under standard cell culture conditions. At 70-80% confluence crizotinib was added to cell culture medium to achieve a designated final concentration at one of nine doses ranging from 0nM to 10,000nM. Cells were incubated for 2 hours with drug, then collected, pelleted, and washed twice with ice cold phosphate-buffered saline (PBS). Whole cell lysates were then harvested, separated and

immunoblotted as previously described (*S3*). The following antibodies were used, according to the supplier's instructions: anti-ALK (1:1,000; Cell Signaling, 3333), anti-phospho-ALK Tyr 1604 (1:1,000, Cell Signaling, 3341), anti-STAT3 (1:1,000; Cell Signaling, 9132), antiphospho-STAT3 Tyr 705 (1:1,000; Cell Signaling, 9145), anti-AKT (1:1,000; Cell Signaling, 9272), anti-phospho-AKT Ser 473 (1:1,000; Invitrogen, 44-621G), anti-p44/42 MAPK (ERK1/2) (1:1,000; Cell Signaling, 4695), anti-phospho-p44/42 MAPK (ERK 1/2) (1:1,000; Cell Signaling, 9101), anti-actin (1:2,000; Santa Cruz, sc-1616).

Quantification of native gels.
Quantification of autophosphorylation progress employed ImageJ (NIH). Background was subtracted using a rollerball radius of 50 pixels. Using the gel analysis tool, the intensity of each band in the native gel was determined and normalized to the total intensity in each respective lane. Data were plotted as fraction of total intensity in each lane vs. reaction time.

Sedimentation equilibrium analytical ultracentrifugation.
ALK-TKD proteins were diluted to 10 and 16.5μM in 25mM HEPES pH 7.4, 150mM NaCl, 2mM DTT, and subjected to sedimentation equilibrium ultracentrifugation at 13,000, 19,000, and 25,000 rpm in a Beckman Optima XL-A ultracentrifuge. Representative data from 13,000 rpm at 10μM are shown in fig. S5. Data are plotted as $\ln(abs_{280})$ vs $(r^2 - r_0^2)/2$, where r is the radial distance of the sample and r_0 is the radial distance of the meniscus. The slope of the line is proportional to the weight-average molecular weight of the species in the sample. Data were analyzed using Sedphat (http://analyticalultracentrifugation.com).

Inhibitor profiling using commercially available kinase inhibitor screens.
Kinase inhibitor screens containing 320 (overlapping) commercially available and well-characterized ATP-competitive inhibitors (Enzo Life Sciences ScreenWell and EMD InhibitorSelect Kinase Inhibitor Libraries 1-3) were used to compare the inhibitor selectivities of wild-type, R1275Q, and F1174L ALK-TKD. ALK TKD (2μM) was incubated with ATP (200μM, corresponding to the approximate $K_{m,ATP}$ of ALK-TKD at 10mM $MgCl_2$) in 96-well format with 50μM of each inhibitor (DMSO only in the negative control wells, or TAE-684 in the positive control wells) in a final reaction volume of 10μl. After incubation at room temperature, reactions were quenched with by adding EDTA to a final concentration of 20mM in 25mM HEPES pH 7.4, 150mM NaCl, 4mM DTT, and spotted onto nitrocellulose membranes in triplicate. Membranes were immunoblotted with anti-phosphotyrosine (PY20, 1:1000, Biomol), detecting with HRP-conjugated α-mouse IgG (1:1000, GE Healthcare).

***In vitro* kinase assays.**
Analysis of substrate phosphorylation by ALK-TKD employed a peptide mimic of the ALK activation loop with sequence: biotin-ARDIYRASYYRKGGCAMLPVK (CanPeptide), referred to as YYY peptide (*S4*). Autophosphorylated ALK-TKD was used at 10nM in these assays, whereas unphosphorylated kinase was studied at 500nM (wild-type) or 50nM (R1275Q and F1174L), concentrations at which spontaneous autophosphorylation is negligible. Assays monitored incorporation of ^{32}P from γ-^{32}P ATP included in trace amounts (~20μCi per experiment) in the reactions. Comparisons with other peptides confirmed that peptide biotinylation does not affect kinetic parameters, and that reaction rates were linear with respect to both enzyme concentration and time under the assay conditions used (fig. S3E,F). Peptide concentrations were determined by absorbance at 280nm using a calculated extinction coefficient $3960 cm^{-1}M^{-1}$.

Assays were performed in 100mM HEPES pH 7.4, 150mM NaCl, 2mM DTT, 10mM $MgCl_2$, and 0.5mg/mL BSA at 25˚C, and were initiated by mixing equal volumes of solutions containing ALK-TKD and substrates respectively (at twice the desired final concentration). For determination of k_{cat} and $K_{m,\ peptide}$, peptide concentration was varied from 0 to 2mM, and ATP was saturating (2mM). For determination of $K_{m,\ ATP}$, peptide was present at a fixed concentration of 1 or 2mM, and ATP was varied from 0.015625 to 2mM. Aliquots were taken at each time point, spotted onto pieces of phosphocellulose paper (Upstate Biotechnology), and immediately quenched with 0.5% phosphoric acid followed by extensive washing and drying with acetone. Incorporated radioactivity was measured by scintillation counting with appropriate background correction. Initial rates (determined at <10% product formation) were calculated using measured apparent γ-^{32}P ATP specific activity, normalized to enzyme concentration, and fit to the Michaelis-Menten equation ($v_o = v_{max}[S]/(K_m+[S])$) using GraphPad Prism 4.0. The enzyme was assumed to have one active site per molecule, therefore $k_{cat} = v_{max}$ at saturating ATP concentrations.

For experiments with added vesicles, which were prepared essentially as described (*S2*), the appropriate amount of vesicle solution (10μM DOGS-NTA-Ni, 100 or 200μM total lipid depending on the molar percentage of DOGS-NTA-Ni used) was added to the 2x protein mixture, and the reaction was performed and processed as above. Control experiments were performed with vesicles containing only dioleoylphosphatidylcholine (200μM total lipid). Enzyme concentration was held fixed at 1μM, with 2mM peptide and 2mM ATP present. Experiments using EGFR-TKD were performed with poly-Glu_4Tyr (Sigma) instead of YYY peptide. Data are reported in Table 1 and tables S2-S5 as the mean of individual experiments (in at least triplicate) ± SEM. *p* values were determined using an unpaired t-test in GraphPad Prism 4.0.

***in vitro* analysis of ALK-TKD inhibition.**

Inhibitor was added to the 2x substrate mixture prior to initiating reactions with ALK-TKD addition, so that final reactions represented a $\log_2$ dilution series from 0 to 25,600nM inhibitor. Protein concentration was held at 50nM, and assays were performed as described above. The concentration of 'YYY' peptide was held fixed at 0.5mM, and ATP was present at 0.2mM or 2mM. Background counts from a no-enzyme control were subtracted, the data were normalized to the 0nM inhibitor reaction and were fit to a sigmoidal dose-response (variable slope) equation in GraphPad Prism 4.0. Data are reported as means of individual experiments (in at least triplicate) ± SEM. *p* values were determined using an unpaired t-test in GraphPad Prism 4.0.

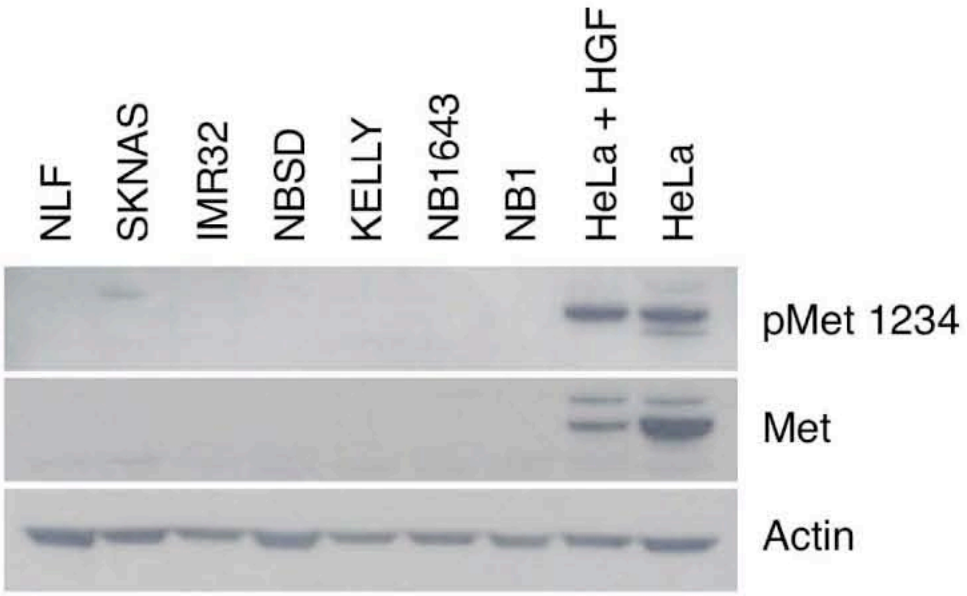

Figure S1. Met and pMet protein expression in neuroblastoma cell lines.
Immunoblots showing native Met and phospho-Met expression in 7 neuroblastoma cell lines, as well as native HeLa cells and HeLa cells treated with hepatocyte growth factor (HGF), the ligand for Met. F1174L-mutated ALK is expressed in NBSD and KELLY cells. R1275Q ALK is expressed in NB1643 cells. NB1 cells have amplified wild-type ALK, and IMR32 cells express wild-type ALK at normal levels. NLF and SKNAS cells harbor no ALK alteration (and do not appear to express ALK).

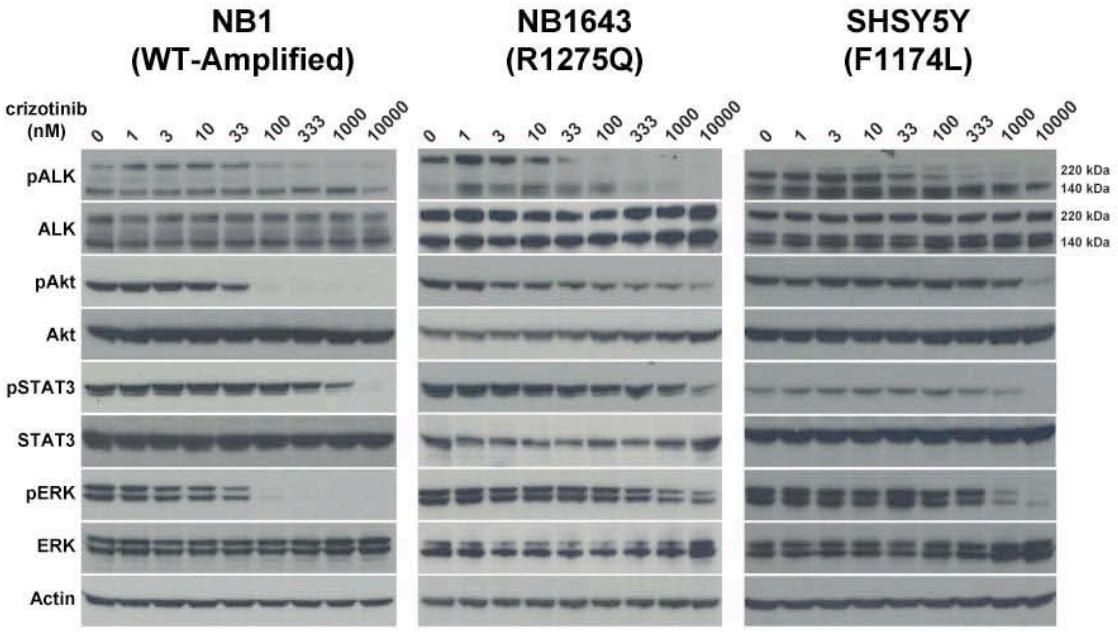

Figure S2. Crizotinib inhibits ALK autophosphorylation and downstream signaling in neuroblastoma cell lines.
Indicated cell lines were treated with the noted crizotinib concentrations and prepared for immunoblotting of whole cell lysates as described in Supplementary Methods. Diminution of pAkt levels approximately parallels that of ALK phosphorylation, with pAkt levels maximally reduced by ~100nM crizotinib in NB1 cells, ~333nM in NB1643 cells, but not until 10,000nM in SH-SY5Y cells. Substantial reduction of pSTAT3 levels requires higher crizotinib concentrations in all three cell lines, and pERK remains detectable even at 10,000nM crizotinib in NB1643 and SH-SY5Y cells. These data are consistent with previous reports that inhibition (or knockdown) of mutated ALK promotes apoptosis of neuroblastoma cell lines (*S5*). The differences in 'sharpness' of pAkt and pERK inhibition between NB1 and NB1643/SH-SY5Y cells appear to reflect receptor expression levels (which are very high in NB1) – and this is currently being investigated further.

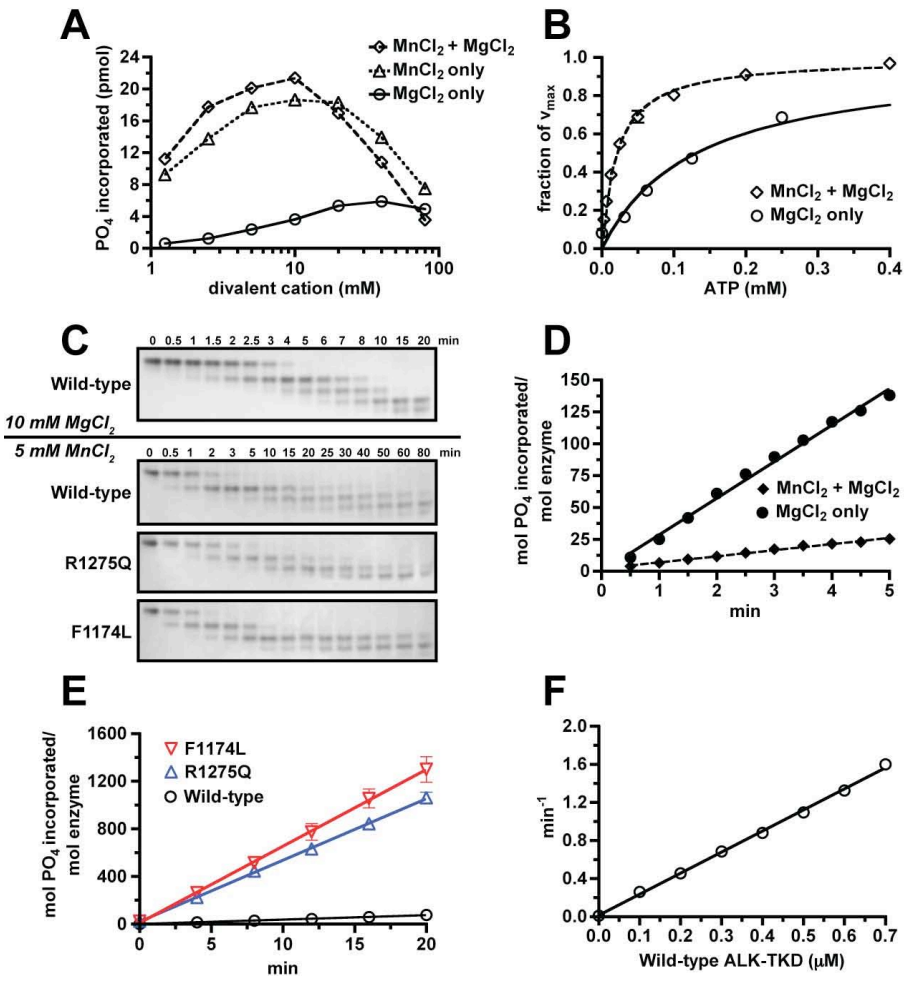

Figure S3. Effects of $MnCl_2$ on ALK-TKD assays.
(**A**) $MnCl_2$ increases the rate of phosphotransfer catalyzed by unphosphorylated ALK-TKD (250nM). Results are representative of two independent experiments performed with 'YFF' peptide (0.5mM) in the presence of 50μM ATP. (**B**) $K_{m,\ ATP}$ for wild-type unphosphorylated ALK-TKD is reduced to 21.3±4.33μM by the addition of 10mM $MnCl_2$ (measured at 1mM 'YYY" peptide, 250nM ALK-TKD, mean ± SEM of four independent experiments), compared with a value of 134±7μM in the presence of 10mM $MgCl_2$ alone (500nM ALK-TKD and 1mM 'YYY' peptide). (**C**) The presence of $MnCl_2$ (5mM) diminishes the apparent activating effects of F1174L and R1275Q mutations, as assessed using native gel electrophoresis to monitor progress of autophosphorylation. In addition, increased basal activity of unphosphorylated ALK-TKD is promoted by $MnCl_2$. All reactions were performed at 37˚C with 10μM ALK-TKD and 1mM ATP. (**D**) $MnCl_2$ (10mM) in addition to $MgCl_2$ (10mM) reduces activity of fully autophosphorylated wild-type ALK-TKD (100nM) using 0.5mM 'YYY' peptide as the phosphoacceptor with 0.2mM ATP present. Results are representative of two independent experiments. (**E**) Initial rates in the final optimized conditions were linear with time, shown here with unphosphorylated proteins (500nM for wild-type, 50nM for R1275Q and F1174L), 2mM 'YYY' peptide, and saturating ATP (2mM). Data are shown as mean ± SEM for at least 3 independent experiments. (**F**) Reaction rates in the final optimized conditions were also linear with enzyme concentration from 0 to 0.7μM for unphosphorylated wild-type ALK-TKD in the presence of 1mM 'YYY' peptide and saturating ATP (1mM).

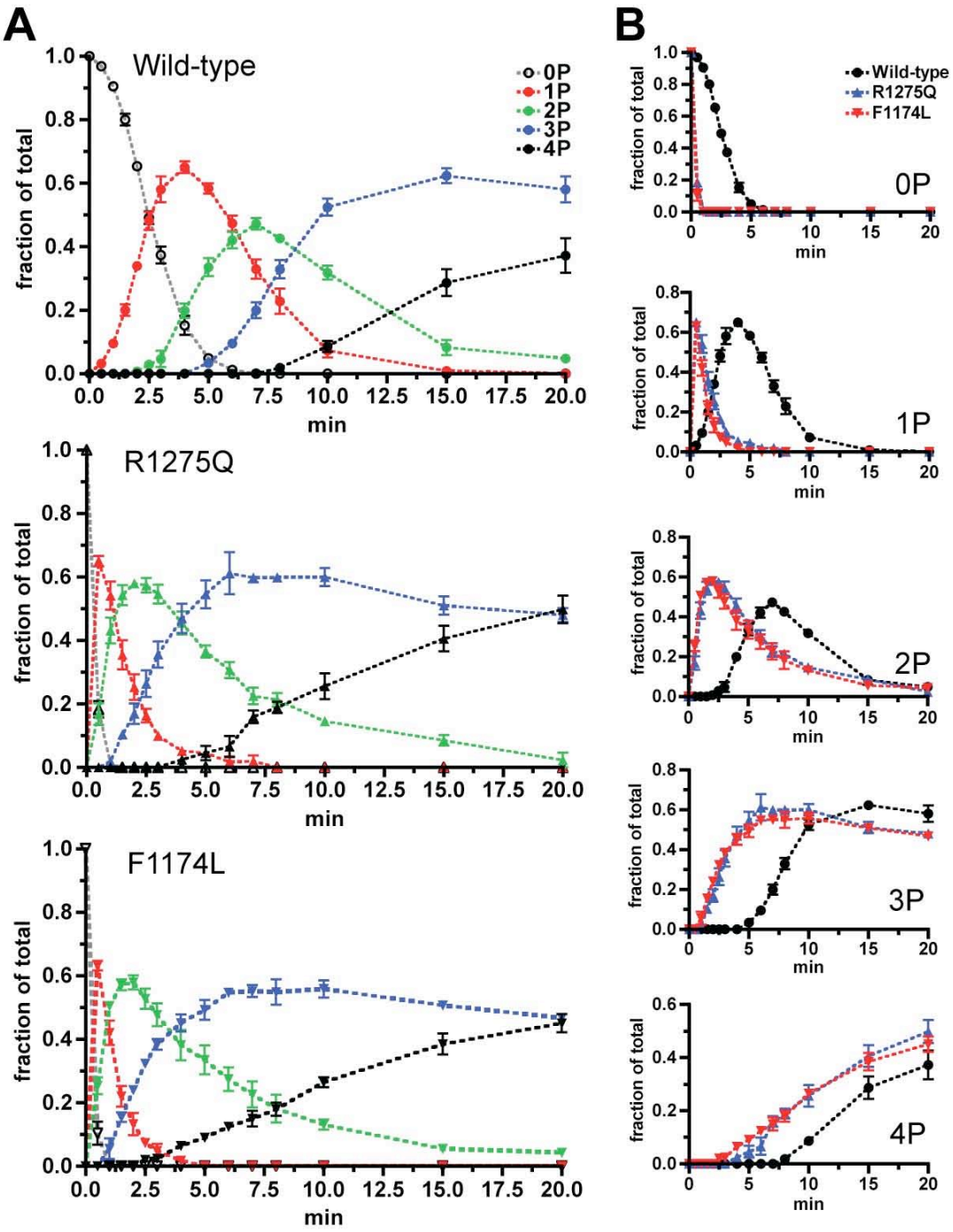

Figure S4. Progress of ALK-TKD autophosphorylation as assessed in native gels. (**A**) Species corresponding to unphosphorylated (0P), singly phosphorylated (1P) and those with 2 (2P), 3 (3P) or 4 (4P) phosphates respectively are tracked with time as denoted in the key – for wild-type, R1275Q, and F1174L ALK-TKD (10μM) with 2mM ATP and 10mM $MgCl_2$ as shown in Fig. 4B. In (**B**), the kinetics of appearance/disappearance of each different phosphospecies are directly compared across the three ALK-TKD variants. All data are shown as mean ± SEM of three independent experiments.

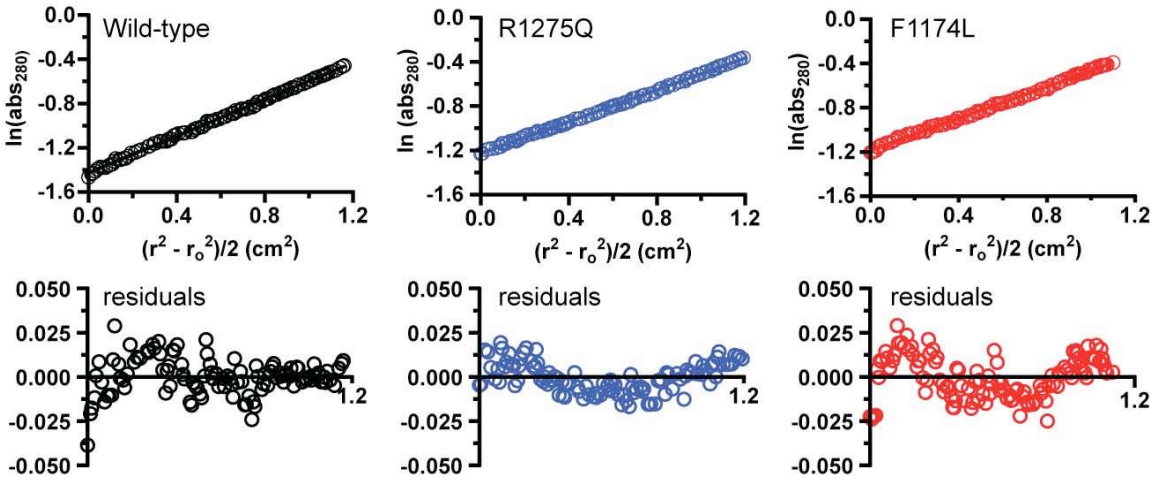

Figure S5. Sedimentation equilibrium ultracentrifugation analysis of ALK-TKD variants. Purified wild-type, F1174L, and R1275Q ALK-TKD were subjected to sedimentation equilibrium analytical ultracentrifugation to measure molecular weight and assess propensity to self-associate (which might be affected by activating mutations). Proteins were centrifuged at three different speeds (13,000, 19,000 and 25,000 r.p.m.) at two different concentrations (10μM and 16.5μM). Efforts were made to globally fit data to models assuming either a single species or self-associating species, and best fits suggested a single species with molecular weight of 38.2kDa (wild-type), 42.4kDa (R1275Q) and 39.6kDa (F1174L). Data from representative experiments performed at 10μM ALK-TKD (at 13,000 r.p.m.) are plotted as $\ln(abs_{280})$ against $(r^2 - r_o^2)/2$. This representation yields a straight line for a single species, with slope proportional to molecular weight. The data (and fits) suggest that – at concentrations in the 10-20μM range – each ALK-TKD variant is monomeric, excluding promotion of dimerization as a mechanism of TKD activation by these neuroblastoma mutations.

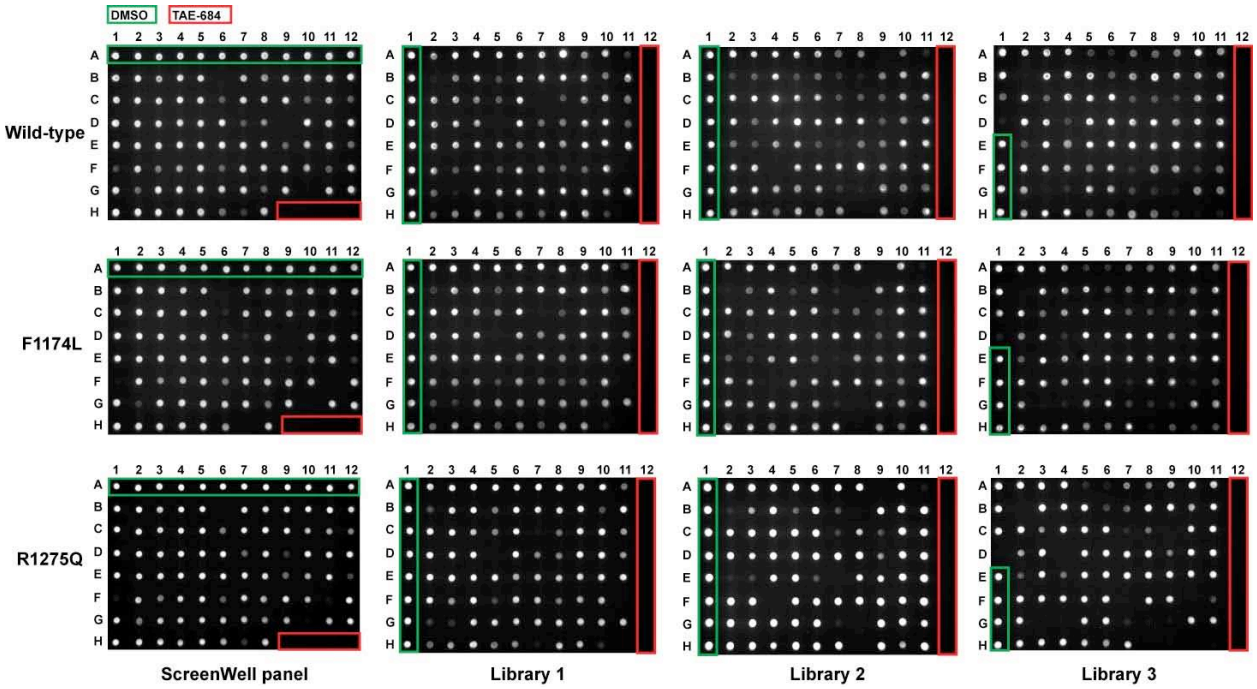

Figure S6. Inhibition of ALK-TKD by inhibitors in the Enzo ScreenWell and EMD InhibitorSelect™ 1-3 collections.
Inhibitor screens using a 96-well plate autophosphorylation assay were performed as described in Supplementary Methods. Several new hits were identified that could be used as scaffolds for future ALK inhibitors. The left-hand arrays correspond to the Enzo ScreenWell panel of 80 kinase inhibitors. Others employed EMD InhibitorSelect Libraries 1-3 as marked. Inhibition was analyzed as described in Supplementary Methods by monitoring autophosphorylation of ALK-TKD variants (2μM) with 0.2mM ATP in anti-pY immunoblots (shown in inverse grey scale). DMSO negative controls are boxed in green. TAE-684 positive inhibition controls are boxed in red. No significant difference in inhibitor selectivity profile is apparent when comparing wild-type, F1174L and R1275Q ALK-TKD, suggesting that the mutations do not substantially alter the nature of the ATP binding site. Components of Enzo Screen-Well™ are listed at http://www.enzolifesciences.com/BML-2832/kinase-inhibitor-library, and those of EMD InhibitorSelect™ are listed at http://www.emdchemicals.com/life-science-research.

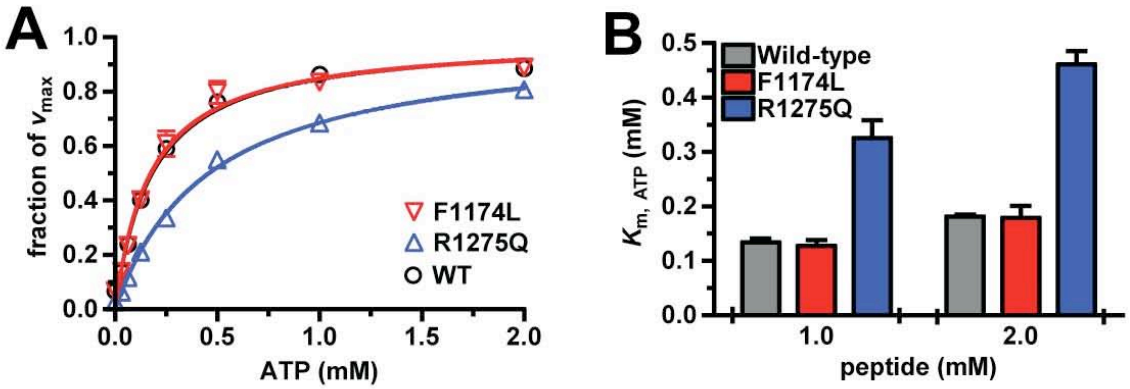

Figure S7. Confirmation of $K_{m, ATP}$ values of ALK-TKD variants at different near-saturating peptide concentrations.
(**A**) Since using a truly saturating level of peptide in $K_{m, ATP}$ assays was not feasible, we determined $K_{m, ATP}$ values for unphosphorylated ALK-TKD variants in the presence of 2mM peptide. Results show a very similar profile to that determined at 1mM peptide (Fig. 5C), with $K_{m, ATP}$ values very slightly increased. The comparative profile for the different ALK-TKD variants (500nM for wild-type, 50nM for mutants) is maintained. (**B**) Direct comparison of $K_{m, ATP}$ values determined in assays employing 1mM and 2mM peptide. Data are shown as mean ± SEM of three independent experiments, and are also shown in table S2.

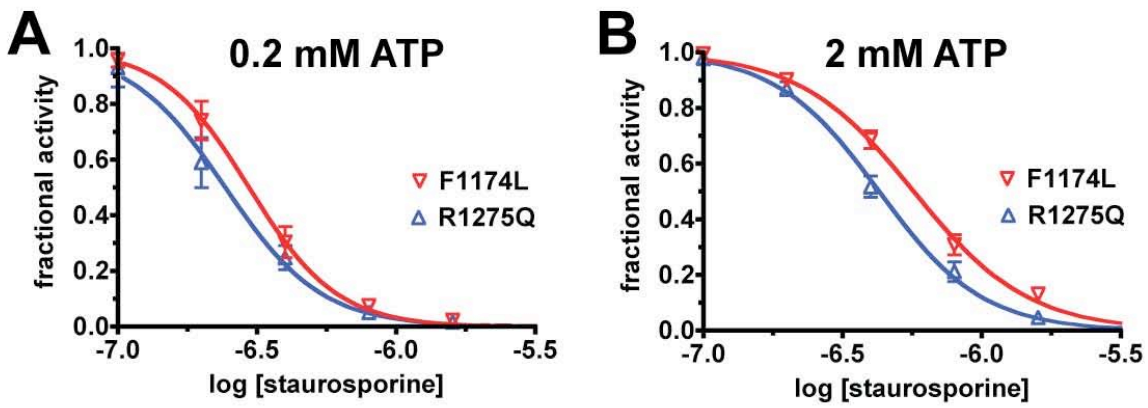

Figure S8. The F1174L mutation also increases IC_{50} for staurosporine inhibition. The ability of staurosporine to inhibit ALK-TKD *in vitro* was analyzed as described for crizotinib in Figure 5 G and H. The IC_{50} for staurosporine inhibition with 0.2mM ATP (**A**) is slightly higher for F1174L-mutated ALK-TKD than for the R1275Q variant (see table S5). As with crizotinib, this difference is enhanced when experiments were performed in the presence of 2mM ATP (**B**), more closely resembling cellular concentrations. All data are shown as the mean ± SEM from at least three independent experiments. The reduced $K_{m,ATP}$ for F1174L ALK-TKD also appears to increase IC_{50} for staurosporine inhibition.

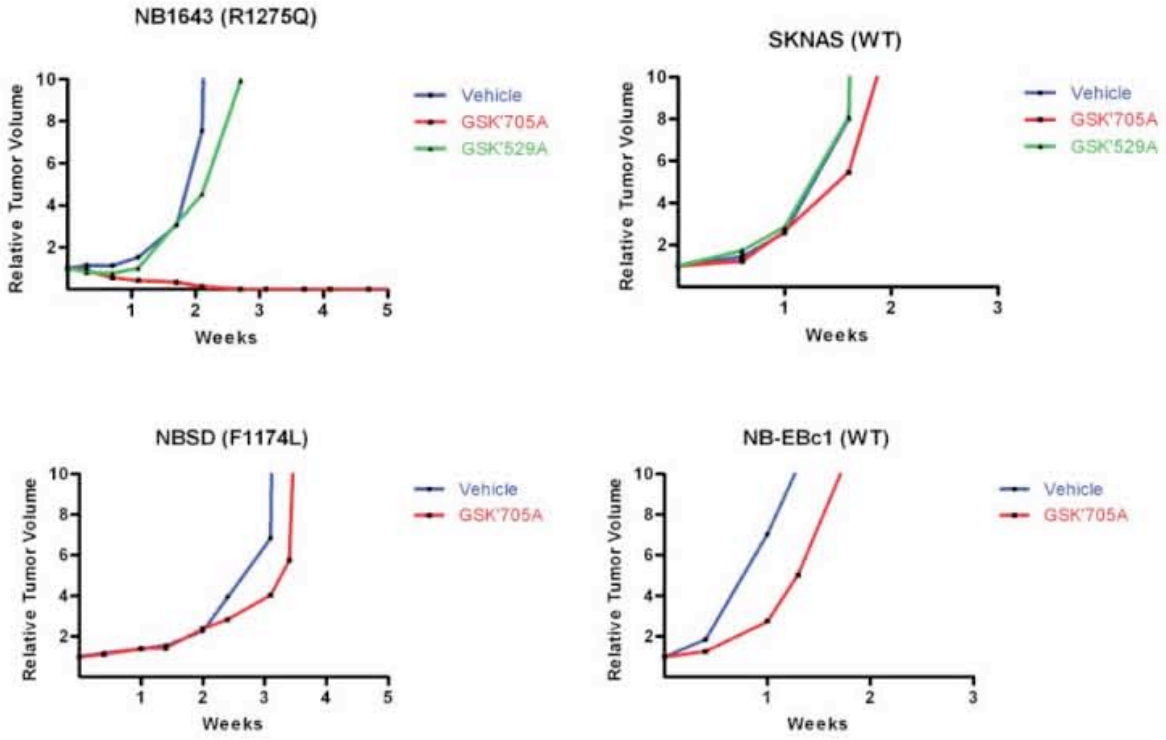

Figure S9. The ALK/IGF1-R inhibitor GSK1838705A promotes regression of xenografts containing R1275Q mutations, but not F1174L or wild-type ALK.
GSK1838705A is another ATP-competitive ALK kinase inhibitor that also inhibits the insulin receptor and IGF1-R (*S6*). GSK1838705A also showed significant single agent activity against the NB1643 cell line (R1275Q) xenografted into CB17 *scid*$^{-/-}$ mice, but not against WT or F1174L xenografts. By contrast, the IGF1-R inhibitor GSK1904529A (*S7*) had no significant effect. Mice were randomized to GSK1838705A 60mg/kg/day once daily, GSK1904529A 30mg/kg/day once daily, or with vehicle (N=10/arm) following xenotransplantation and establishment of a tumor at 200 mm^3. GSK1838705A caused complete regression of NB1643 xenografts within two weeks. Dosing was continued for a further two weeks, during which time tumors remained in macroscopic remission.

Table S1. Effect of siRNA knockdown of ALK and Met on proliferation of neuroblastoma cell lines.

	Relative proliferation			
	KELLY (F1174L)	*EBC1 (WT)*	*SKNAS (WT)*	*NLF (WT)*
ALK siRNA	0.190	0.728	0.930	0.729
Met siRNA	0.772	0.421	0.797	0.439

Proliferation of the KELLY cell line harboring a F1174L mutation is inhibited by siRNA knockdown of ALK, but shows less inhibition with Met knockdown. The remaining three cell lines harbor wild-type normal copy number ALK. Cells were plated overnight and then transfected in triplicate with a pool of four siRNA targeting each kinase (Thermo Scientific Kinase siGenome Library), with positive (siPLK1) and negative (GAPD) controls. Substrate adherent growth was monitored for 100 hours using the Roche xCELLigence system. The area under the curve was calculated for each siRNA triplicate and mock transfection. % relative growth = AUC of the siKinase/AUC siControl.

Table S2. Dependence of K_m, ATP on peptide concentration for unphosphorylated ALK-TKD variants. (Data are shown as mean ± SEM for at least 3 independent experiments).

kinase	$K_{m,\ ATP}$, *1mM peptide (mM)*	$K_{m,\ ATP}$, *2mM peptide (mM)*
WT	0.134 ± 0.007	0.181 ± 0.004
R1275Q	0.326 ± 0.033	0.460 ± 0.024
F1174L	0.127 ± 0.011	0.179 ± 0.022

Table S3. Crizotinib inhibition of unphosphorylated ALK-TKD *in vitro* at two different ATP concentrations. (Data are shown as mean ± SEM for at least 3 independent experiments).

kinase	IC_{50}, *2 mM ATP (nM)*	IC_{50}, *0.2 mM ATP (nM)*
WT	147 ± 6	--
R1275Q	84.6 ± 8.0	80.4 ± 4.8
F1174L	130 ± 10	88.5 ± 6.4

Table S4. IC_{50} measurements for crizotinib inhibition of phosphorylated ALK-TKD variants (10nM).

kinase	*IC_{50} (nM)*
pWT	93.3
pR1275Q	67.3
pF1174L	111.0

Table S5. IC_{50} measurements for *in vitro* staurosporine inhibition of ALK-TKD variants. (Data are shown as mean ± SEM for at least 3 independent experiments).

kinase	*IC_{50}, 0.2mM ATP (nM)*	*IC_{50}, 2.0mM ATP (nM)*
R1275Q	227 ± 32.0	404 ± 25.6
F1174L	271 ± 26.7	545 ± 39.5

Table S6. IC_{50} measurements for inhibition of neuroblastoma cell lines by the ALK/InsR/IGF1-R inhibitor GSK1838705A.

ALK status	*Cell line*	*IC_{50} for GSK1838705A(nM)*
R1275Q	NB1643	124
F1174L	NBSD	10000
F1174L	KELLY	605
F1174L	SH-SY5Y	781
WT amp	IMR5	7911
WT,	SKNFI	10000
normal	NGP	10000
copy	NB16	10000
number	NLF	10000

GSK1838705A is an ATP-competitive inhibitor of the ALK, insulin receptor, and IGF1-R tyrosine kinases GSK1838705A (*S6, S8*).

Supplementary References

S1. Z. Y. Zhang, J. C. Clemens, H. L. Schubert, J. A. Stuckey, M. W. Fischer, D. M. Hume, M. A. Saper, J. E. Dixon, Expression, purification, and physicochemical characterization of a recombinant Yersinia protein tyrosine phosphatase. *J. Biol. Chem.* **267**, 23759-23766 (1992).

S2. X. Zhang, J. Gureasko, K. Shen, P. A. Cole, J. Kuriyan, An allosteric mechanism for activation of the kinase domain of epidermal growth factor receptor. *Cell* **125**, 1137-1149 (2006).

S3. Y. P. Mossé, M. Laudenslager, L. Longo, K. A. Cole, A. Wood, E. F. Attiyeh, M. J. Laquaglia, R. Sennett, J. E. Lynch, P. Perri, G. Laureys, F. Speleman, C. Kim, C. Hou, H. Hakonarson, A. Torkamani, N. J. Schork, G. M. Brodeur, G. P. Tonini, E. Rappaport, M. Devoto, J. M. Maris, Identification of ALK as a major familial neuroblastoma predisposition gene. *Nature* **455**, 930-935 (2008).

S4. A. Donella-Deana, O. Marin, L. Cesaro, R. H. Gunby, A. Ferrarese, A. M. Coluccia, C. J. Tartari, L. Mologni, L. Scapozza, C. Gambacorti-Passerini, L. A. Pinna, Unique substrate specificity of anaplastic lymphoma kinase (ALK): development of phosphoacceptor peptides for the assay of ALK activity. *Biochemistry* **44**, 8533-8542 (2005).

S5. R. E. George, T. Sanda, M. Hanna, S. Frohling, W. Luther, 2nd, J. Zhang, Y. Ahn, W. Zhou, W. B. London, P. McGrady, L. Xue, S. Zozulya, V. E. Gregor, T. R. Webb, N. S. Gray, D. G. Gilliland, L. Diller, H. Greulich, S. W. Morris, M. Meyerson, A. T. Look, Activating mutations in ALK provide a therapeutic target in neuroblastoma. *Nature* **455**, 975-978 (2008).

S6. P. Sabbatini, S. Korenchuk, J. L. Rowand, A. Groy, Q. Liu, D. Leperi, C. Atkins, M. Dumble, J. Yang, K. Anderson, R. G. Kruger, R. R. Gontarek, K. R. Maksimchuk, S. Suravajjala, R. R. Lapierre, J. B. Shotwell, J. W. Wilson, S. D. Chamberlain, S. K. Rabindran, R. Kumar, GSK1838705A inhibits the insulin-like growth factor-1 receptor and anaplastic lymphoma kinase and shows antitumor activity in experimental models of human cancers. *Mol. Cancer Ther.* **8**, 2811-2820 (2009).

S7. P. Sabbatini, J. L. Rowand, A. Groy, S. Korenchuk, Q. Liu, C. Atkins, M. Dumble, J. Yang, K. Anderson, B. J. Wilson, K. A. Emmitte, S. K. Rabindran, R. Kumar, Antitumor activity of GSK1904529A, a small-molecule inhibitor of the insulin-like growth factor-I receptor tyrosine kinase. *Clin. Cancer Res.* **15**, 3058-3067 (2009).

S8. E. Ardini, P. Magnaghi, P. Orsini, A. Galvani, M. Menichincheri, Anaplastic Lymphoma Kinase: role in specific tumours, and development of small molecule inhibitors for cancer therapy. *Cancer Lett.* **299**, 81-94 (2010).